24th COBEM - 2017

24th ABCM International Congress of Mechanical Engineering
December 3-8, 2017, Curitiba, PR, Brazil

COBEM-2017-0579
SIMULATION OF A 2-D PULSATILE FLOW IN A BIFURCATED GEOMETRY USING OPEN SOURCE SOFTWARE

Gustavo P. V. Almeida
Instituto Tecnológico de Aeronáutica - ITA
gupalmeida@gmail.com

João Luiz F. Azevedo
Instituto de Aeronáutica e Espaço - IAE
joaoluiz.azevedo@gmail.com

Abstract. *Numerical simulations of pulsatile flow have been largely applied in the field of hemodynamics to analyze the behavior of blood flow within a vessel. The present work applies these methodologies for simulating the effects of pulsatile flow in a bifurcated geometry. The simulations are performed for a general incompressible Newtonian fluid using an open source CFD package in both steady and transient regimes. A large region of recirculation is observed in the steady flow whereas the pulsatile case attenuates these variations of velocity at the bifurcation location due to the time-dependent velocity sinusoidal wave frequency.*

Keywords: *CFD, Bifurcation, Pulsatile Flow, Incompressible Flow, Open Source Software*

1. INTRODUCTION

Over the past years, computational simulations of fluid flows have been conducted for a substantial number of applications. Among these numerous fields of interest one has recently gained a great importance. The studies of the blood flow behavior within arteries in the field of hemodynamics have increased in the last decade. Great effort has been spent in the attempt of correlating the flow parameters with potential cardiovascular diseases such as arterial hypertension and aneurysms rupture, among others (Cebral *et al.*, 2007). Velocity fields, pressure and shear stresses distribution are the most studied parameters among the scientific community.

Numerical simulations of both steady and transient flow regimes have been exhaustively explored in order to validate computational results with medical data. This effort of getting high-fidelity models is driven by the idea of using the computational results as support to medical decision making as well as medical diagnostics (Wong and Poon, 2011). More specific studies have applied these simulations in order to get patient-specific Computational Fluid Dynamics (CFD) results to use them as a part of the patient management. Thus, the use of CFD applied to hemodynamics has gained a great importance worldwide. Despite the high-accuracy results obtained so far, there is still a question of whether these models may be indeed used to predict any risky behavior of the blood flow prior to any medical treatment (Cebral *et al.*, 2007).

A general and common approach for modeling the blood flow in a vessel found in literature is assuming the blood as a Newtonian fluid and the blood vessel as a rigid body to simplify the simulations. Moreover, the attention is directed to flow regions with a significant variation of the flow parameters - mainly the shear stresses distribution. It is believed these fluctuations in the shear stress values along the flow path may lead to the appearance of some cardiovascular diseases such as aneurysms and stenosis. These fluctuations appear mainly due to transient effects on the flow and, therefore, it is quite important to consider the unsteady flow once the heart rate cycle of contracting and relaxing induces the so called pulsatile flow (Favero *et al.*, 2010a,b). Notwithstanding, the influence of the geometry of the blood vessels on the flow parameters is also a topic of great interest. Researchers believe the bifurcations found in the blood network present great influence on the shear stress distribution as blood is flowing (Shaik *et al.*, 2006).

The present work focus on analyzing the influence of Reynolds number of an incompressible Newtonian fluid flowing through a bifurcation for both steady and pulsatile flow regimes. The model walls are assumed as rigid for simplification of the current simulations. The results are presented for values of Reynolds number of 100, 200 and 300 as found in literature for the application of interest (Pinto *et al.*, 2013; Shaik *et al.*, 2006).

2. METHODOLOGY

The methodology followed is be divided basically into two stages: I - mathematical modeling of the governing equations of the flow; II - computational procedure - (a) computational mesh generation and (b) numerical solution using a CFD solver. Each one of these stages will be briefly described hereafter.

The choice of an open source code for solving the fluid motion problem is due to its wide applicability and ease to adapt the code to any user need. Interestingly, previous studies have shown a high-fidelity between Open Source CFD software and Commercial CFD software (Favero *et al.*, 2010a; Pinto *et al.*, 2013).

2.1 Theoretical Model

In general, any flow may described by the Navier-Stokes equations. When dealing with an incompressible Newtonian fluid its density is assumed to be a constant and, without heat exchange, the equation of energy may be neglected. Hence, for an incompressible Newtonian fluid flowing throughout an isothermal mean the flow governing equations become:

$$\nabla.\vec{u} = 0 \tag{1}$$

and

$$\frac{\partial(\rho\vec{u})}{\partial t} + \nabla.(\rho\vec{u} \times \vec{u}) = -\nabla p + \nabla\bar{\bar{\tau}}, \tag{2}$$

where $\vec{u}$ is the velocity vector, ρ is the fluid density and $\bar{\bar{\tau}}$ is the stress tensor. The stress tensor for a Newtonian fluid is given by:

$$\bar{\bar{\tau}} = \mu\nabla\vec{u} + \lambda(\nabla.\vec{u})^T\bar{\bar{I}}, \tag{3}$$

with $\lambda = \frac{2}{3}\mu$, where μ is the dynamic viscosity of the fluid and $\bar{\bar{I}}$ is the identity tensor.

As the fluid density is a constant it may be carried out from the derivatives. Following this procedure and dividing all the terms by the density, Eq. 2 becomes:

$$\frac{\partial\vec{u}}{\partial t} + \nabla.(\vec{u} \times \vec{u}) = -\nabla\left(\frac{p}{\rho}\right) + \nabla\bar{\bar{\tau}}_{incompressible}, \tag{4}$$

where the ratio p/ρ is referenced to as kinematic pressure in OpenFOAM manuals (OpenCFD, 2016). In order to ease the reading the authors decided to reference to this term as pressure only.

2.2 Computational Procedure

The computational procedure starts by the geometry meshing, which consists on the transformation of the physical domain into a computational grid. The chosen geometry is a general case bifurcated pipe whose dimensions were set to a constant circular cross section of 5 mm, which is a common value found in literature (Favero *et al.*, 2010a; Pinto *et al.*, 2013; Shaik *et al.*, 2006) for arteries. The fluid enters the domain through the parent section of the pipe e exits it throughout its two daughter branches, as depicted in Fig. 1.

The simulations are conducted using Open source Field Operation And Manipulation (OpenFOAM) tools as described hereafter. OpenFOAM is a set of libraries written in C++ used to perform operations with scalar, vector and tensorial fields (Weller *et al.*, 1998).

2.2.1 Computational Mesh

The computational grid is made over a three-dimensional geometry, however, the results are obtained only for a XY plane cut of the proposed geometry. OpenFOAM reads a 3-D mesh even in case the simulation is conducted for a 2-D case. The third dimension is disregarded from the simulation by imposing a boundary condition whose normals are aligned to the geometric directions that are not considered as part of the solution (OpenCFD, 2016).

The final mesh was generated using the open source software Gmsh (Geuzaine and Remacle, 2017). The total number of elements in the final mesh was $180,413$ of . The computation grid on the bifurcation region is depicted in Fig. 2.

2.2.2 Numerical Solution

The open source code works with the Finite Volume Method (FVM) (Moukalled *et al.*, 2016) for discretization of the flow governing equations. There are several solvers available in OpenFOAM library. The icoFoam for example is a solver used to simulate incompressible Newtonian fluid flowing in laminar regime whereas pimpleFoam is one of many choices for incompressible fluid, offering the possibility of turning on a turbulence model in case of working with turbulent flows.

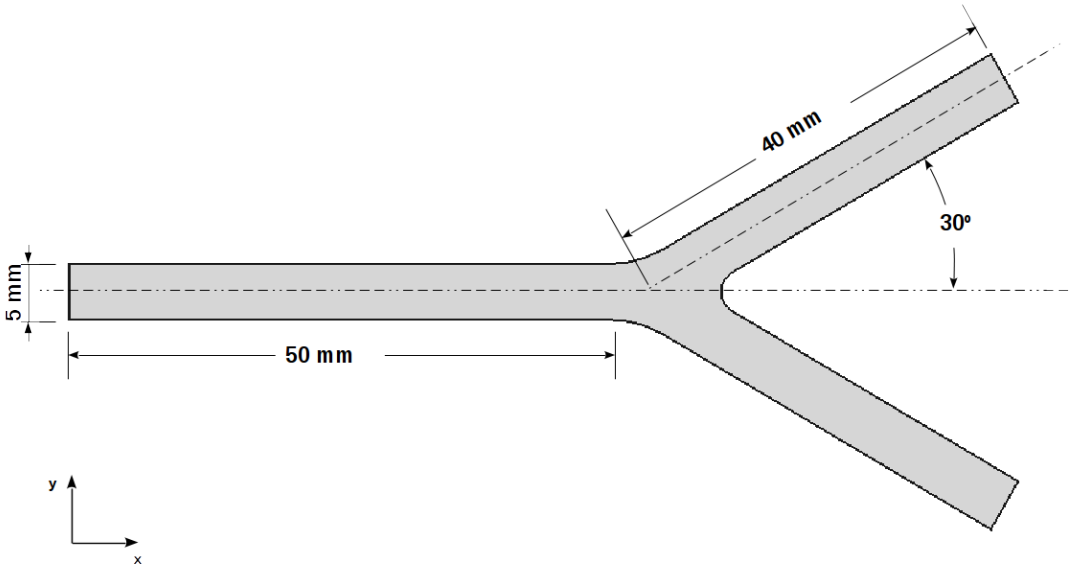

Figure 1: Bifurcated geometry dimensions.

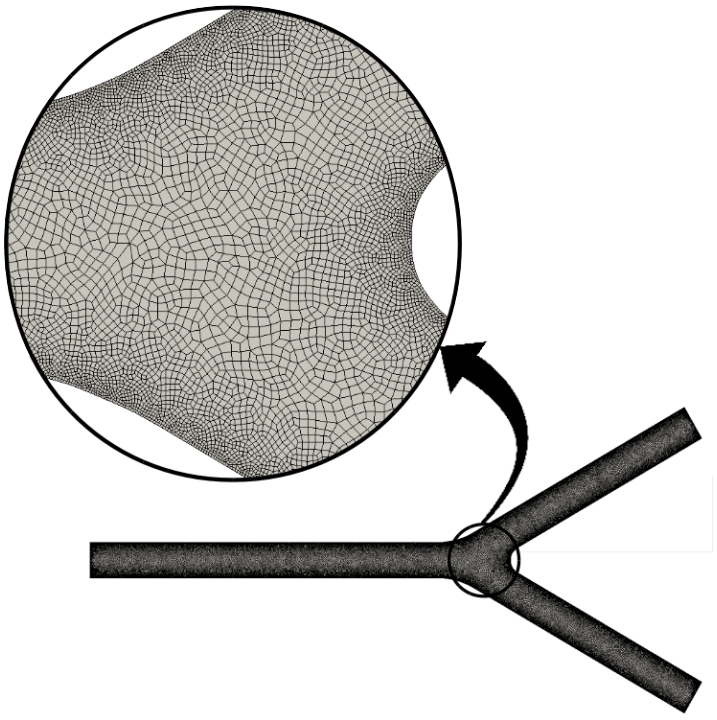

Figure 2: Computational mesh on the bifurcation region.

Reynolds Averaged Navier-Stokes (RANS) and Large Eddy Simulation (LES) models are available for pimpleFoam. The user is also allowed to choose to turn off the turbulence models and work with laminar flow using pimpleFoam as well. Therefore, pimpleFoam offers a wide variety of models.

The process of discretization together with the chosen turbulence model (RANS, LES, laminar) results in a system of equations to be solved later in the process. Hence, the resulting system of equations being solved by OpenFOAM depends on the choice of the solver. The pimpleFoam was chosen due to its wide variety of applicability.

The pimpleFoam is a solver which uses the so called PIMPLE algorithm which is a combination of Pressure-Implicit-Split-Operator (PISO) and Semi-Implicit-Method-of-Pressure-Linked-Equations (SIMPLE) algorithms. Basically the PIMPLE algorithm solves the pressure-momentum coupling allowing one to use bigger time steps for a transient flow without major effects on the simulation accuracy. This is achieved by relaxing the solution at each time step in the attempt of finding a pseudo steady-state solution. After the simulation control parameters (i.e., tolerances, number of iterations, etc) are satisfied the simulation goes on in time and the process repeats itself (Moukalled *et al.*, 2016).

The numerical schemes for both temporal and spatial terms of the discretized equations as well as simulation control parameters are defined into OpenFOAM dictionaries. The authors have chosen a simple Gauss linear scheme for spatial derivatives with non-nonorthogonal correction and a second order backward implicit method for time derivatives, both of which are already available in OpenFOAM library. The simulations were conducted on OpenFOAM version v4.1.

The boundary conditions are defined as a fixed value of the mean flow velocity at the inlet and fixed value of pressure at the outlet for the steady case. The outflow velocity and inflow pressure are then defined so that the flux at each boundary is respected. A schematic of the imposition of boundary conditions is shown in Fig. 3a. For the transient case a

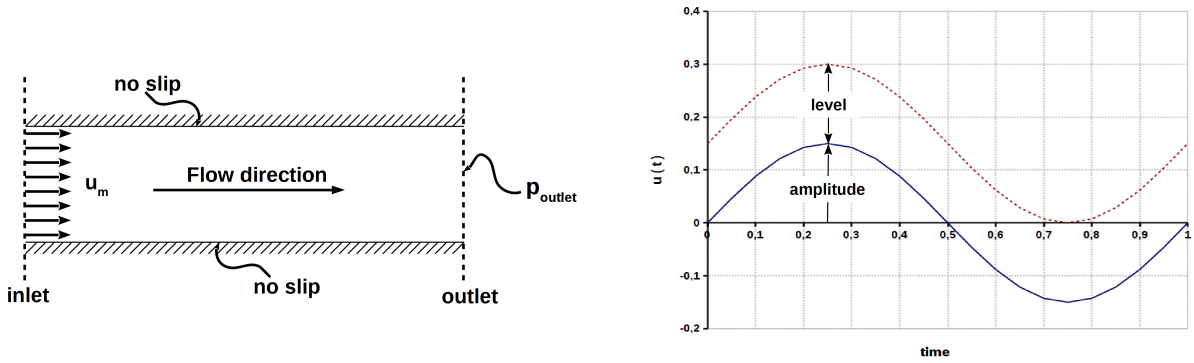

(a) Velocity and pressure BCs. (b) Sinusoidal wave.

Figure 3: Boundary conditions.

time-dependent velocity was set according to the following expression:

$$u(t) = u_m.sin(2\pi t f) + l \tag{5}$$

where u_m is the mean velocity of the full developed velocity profile in the pipe - or the wave amplitude, f is the wave frequency, t is the simulation runtime and l is the wave level. The example of a wave with the form of Eq. 5 is depicted in Fig. 3b. Probes have been placed along stations A, B and C over the geometry as shown in Fig. 4.

3. RESULTS AND DISCUSSIONS

An analysis of the fully developed velocity profile obtained by numerical simulations is done as a sanity check. Figure 5 shows the comparison of the velocity profile at probe station A along the pipe parent branch for both theoretical and numerical results. The numerical results of the parabolic velocity distribution along the parent branch diameter matched the theoretical curve.

The contours of velocity magnitude are depicted in Fig. 6. Figures 6a, 6b and 6c are the results for $Re = 100$, $Re = 200$ and $Re = 300$, respectively. The flow split at the bifurcation for the daughter branches presented the same parabolic distribution, however, with their mean velocity being half of the mean velocity found in the parent branch, as expected.

A small area of recirculation in the flow is observed at low Reynolds number near the region where the parent branch bifurcates onto its two daughter branches. The consequence of increasing Reynolds number is the growth of such recirculation area. These regions are subjected to a significant fluctuation on the values of velocity and, consequently, shear stresses.

The results of velocity distribution for the pulsatile case are presented at four different time instants. The sinusoidal wave amplitude, frequency and level were adjusted so that the maximum and minimum values of the sinusoidal wave are 0.6 m/s and 0 m/s, respectively. Figures 7a and 7b show the velocity profiles at probe stations A and B. Station C presents the same velocity distribution as the one displayed for station B due to symmetry.

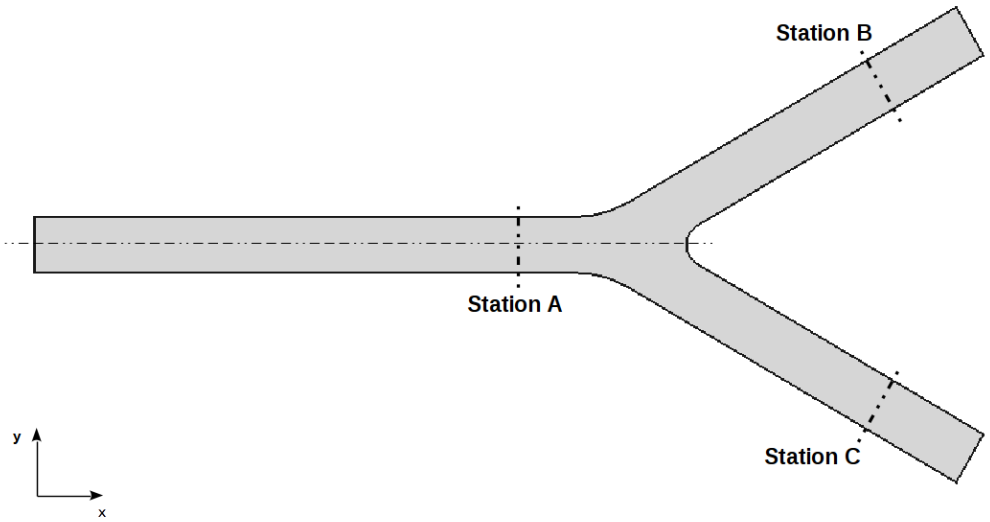

Figure 4: Probing stations over the geometry.

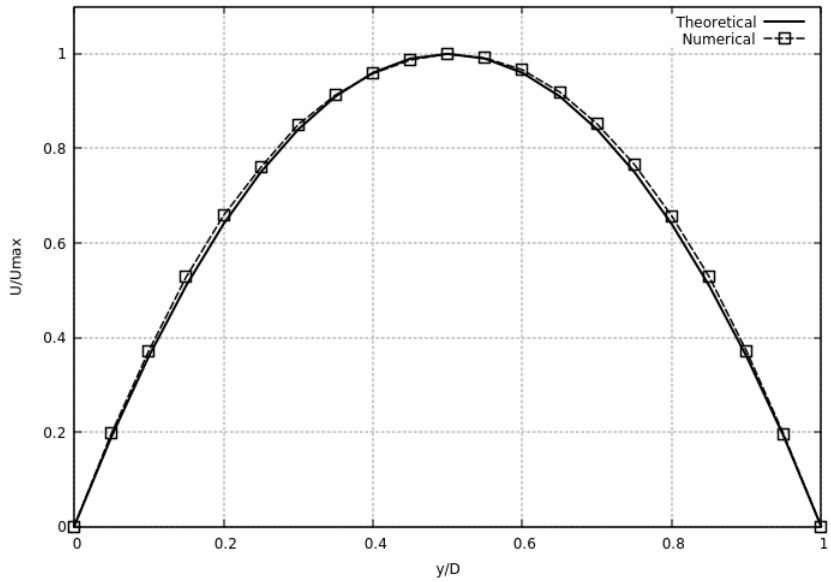

Figure 5: Velocity profile at probe station A along the parent branch for both theoretical and numerical results.

The parent branch shows a higher sensibility in relation to the variation of the time-dependent velocity imposed as a sinusoidal wave at the inlet. The parabolic profile, however, remains the same as the steady case except for the magnitude. The effects of the pulsatile flow are observed at the recirculation regions as well. There is an attenuation on the flow recirculation due to the wave pulse frequency.

4. CONCLUSIONS

OpenFOAM has proven high fidelity comparing the numerical results with the analytical velocity profile for steady cases. The appearance of recirculation in the flow originated from increasing Reynolds number points out to a region of interest when studying the variation of shear stresses. These variations are believed to be related to the appearance of some cardiovascular diseases such as aneurysms and, therefore, attention shall be given to these regions when studying the blood flow behavior in bifurcations.

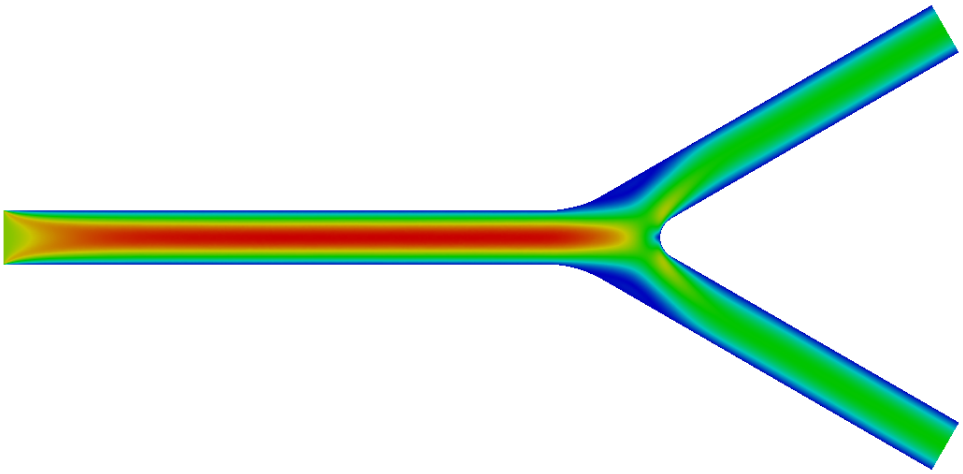

(a) Velocity contour for Re = 100.

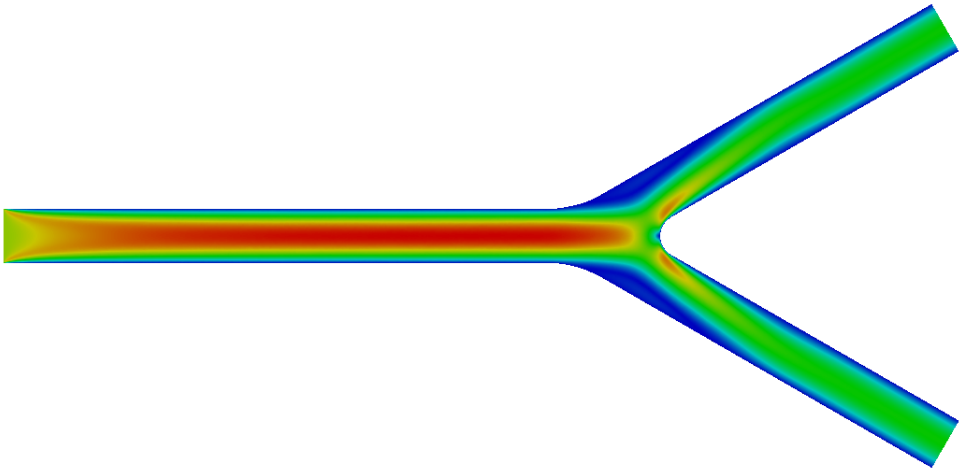

(b) Velocity contour for Re = 200.

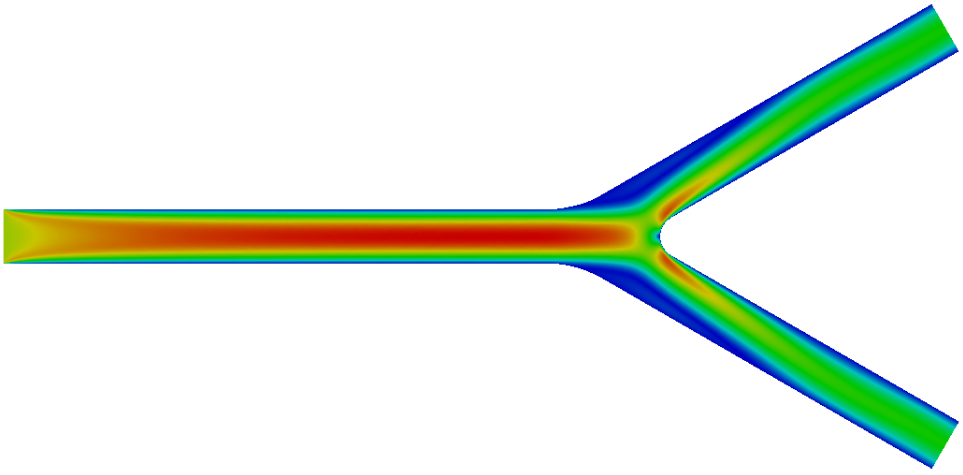

(c) Velocity contour for Re = 300.

Figure 6: Velocity magnitude contours for steady solution.

The results for transient flow have shown that the parent branch is more sensible to the time-dependent sinusoidal wave of velocity imposed at the inlet. The velocity distribution remained with the parabolic profile as for the steady case. The

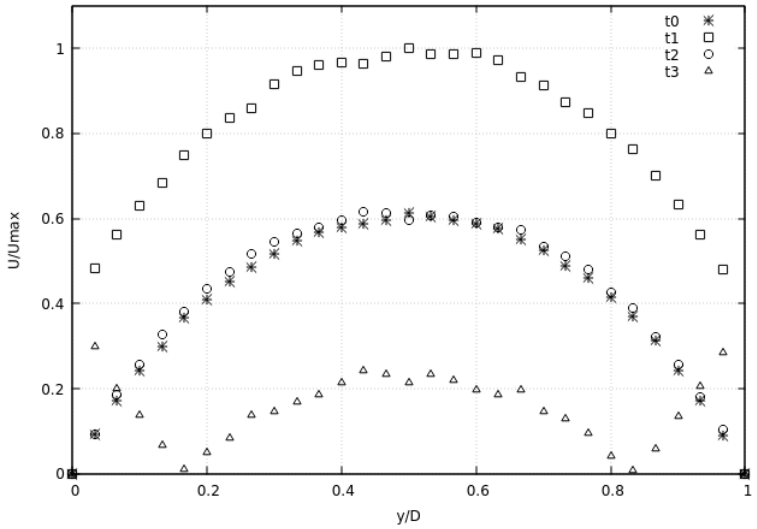

(a) Pulsatile velocity profile at probe station A.

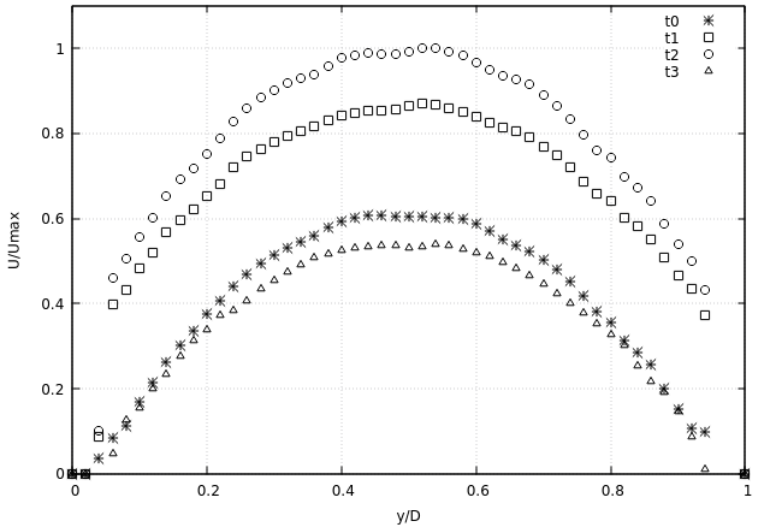

(b) Pulsatile velocity profile at probe station B.

Figure 7: Pulsatile velocity profiles at the probing stations.

recirculation regions have also been impacted. The large area of recirculation observed in the steady cases was attenuated in the pulsatile case due to the pulse wave frequency. Hence, it is easy to conclude that it is necessary to have an exact human pulse wave to study in details the appearance of recirculation regions.

5. ACKNOWLEDGEMENTS

The authors gratefully acknowledge the partial support for this research provided by Conselho Nacional de Desenvolvimento Científico e Tecnológico, CNPq, under the Research Grants No. 309985/2013-7, No. 400844/2014-1 and No. 443839/2014-0. The authors are also indebted to the partial financial support received from Fundação de Amparo à Pesquisa do Estado de São Paulo, FAPESP, under the Research Grant No. 2013/07375-0. The authors wish to thank further Fundação Coordenação de Aperfeiçoamento de Pessoal de Nível Superior, CAPES, which provided a doctoral scholarship for the first author.

6. REFERENCES

Cebral, J.R., Pergolizzi Jr., R. S. and Putman, C.M., 2007. "Computational fluid dynamics modeling of intracranial aneurysms:: Qualitative comparison with cerebral angiography". *Academic Radiology*, Vol. 14, pp. 804 – 813.

Favero, J.L., Secchi, A.R., Cardozo, N.S.M. and Jasak, H., 2010a. "Viscoelastic flow analysis using the software OpenFOAM and differential constitutive equations". *Journal of Non-Newtonian Fluid Mechanics*, Vol. 165, p. 23–24.

Favero, J., Secchi, A., Cardozo, N. and Jasak, H., 2010b. "Viscoelastic fluid analysis in internal and in free surface flows using the software OpenFOAM". *Computers and Chemical Engineering*, Vol. 34, pp. 1984 – 1993.

Geuzaine, C. and Remacle, J.F., 2017. *Gmsh Reference Manual*.

Moukalled, F., Mangani, L. and Darwish, M., 2016. *The Finite Volume Method in Computational Fluid Dynamics - An Advanced Introduction with OpenFOAM® and Matlab®*. Springer International Publishing Switzerland, Switzerland.

OpenCFD, 2016. *OpenFOAM User Guide Manual*. OpenCFD Limited.

Pinto, S., Doutel, E., Campos, J. and Miranda, J., 2013. "Blood analog fluid flow in vessels with stenosis: Development of an OpenFOAM code to simulate pulsatile flow and elasticity of the fluid". *APCBEE Procedia*, Vol. 7, pp. 73–79.

Shaik, E., Hoffmann, K.A. and Dietiker, J.F., 2006. "Numerical flow simulations of blood in arteries". In *44th AIAA Aerospace Sciences Meeting and Exhibit, Applied CFD I*. Reno, Nevada.

Weller, H.G., Tabor, G., Jasak, H. and Fureby, C., 1998. "A tensorial approach to computational continuum mechanics using object-oriented techniques". *Computers in Physics*, Vol. 12, pp. 620–631.

Wong, G.K. and Poon, W., 2011. "Current status of computational fluid dynamics for cerebral aneurysms: The clinician's perspective". *Journal of Clinical Neuroscience*, Vol. 18, pp. 1285 – 1288.

7. RESPONSIBILITY NOTICE

The authors are solely responsible for the printed material included in this paper.